energies

MDPI

Article

An Accurate Method for Delay Margin Computation for Power System Stability

Ashraf Khalil * and **Ang Swee Peng**

Electrical and Electronic Engineering Department, Universiti Teknologi Brunei, Bandar Seri Begawan BE1410, Brunei Darussalam; sweepeng.ang@utb.edu.bn

* Correspondence: ashraf.sulayman@utb.edu.bn; Tel.: +673-246-1029

Received: 7 October 2018; Accepted: 22 October 2018; Published: 11 December 2018

Abstract: The application of the phasor measurement units and the wide expansion of the wide area measurement units make the time delay inevitable in power systems. The time delay could result in poor system performance or at worst lead to system instability. Therefore, it is important to determine the maximum time delay margin required for the system stability. In this paper, we present a new method for determining the delay margin in the power system. The method is based on the analysis in the s-domain. The transcendental time delay characteristics equation is transformed to a frequency dependent equation. The spectral radius is used to find the frequencies at which the roots cross the imaginary axis. The crossing frequencies are determined through the sweeping test and the binary iteration algorithm. A single machine infinite bus system equipped with automatic voltage regulator and power system stabilizer is chosen as a case study. The delay margin is calculated for different values of the power system stabilizer (PSS) gain, and it is found that increasing the PSS gain decreases the delay margin. The effectiveness of the proposed method has been proved through comparing it with the most recent published methods. The method shows its merit with less conservativeness and fewer computations.

Keywords: communication time delays; delay margin; delay dependent stability; excitation control; power system; sweeping test

1. Introduction

A time delay exists inherently in many dynamical systems. In a power system, the time delay is inevitable, especially if open communications are adopted [1]. Time delays could arise in power systems for different reasons and their magnitudes depend on the type of the communication link, for example, telephone lines, fiber-optics, power lines, and satellites [2]. Additionally, the advances and the wide expansion of the phase measurement units (PMUs) and the wide area measurements systems (WMAS) make the time delay unavoidable in the power system. In power systems, the time delay for the feedback signals is in the order of 100 ms [3]. The time delays in the communication links induced into the power systems are within the range of a few milliseconds to one hundred milliseconds depending on the communication network type used, the transmission protocol, network load, and other factors [3,4]. The time delay is in the order of a few seconds in the load frequency control systems [5,6]. The presence of the time delay could lead to poor system performance, or at worst, system instability.

Extensive research has been carried out in the last few decades to tackle the problems associated with the delay in the power system, the readers can refer to References [7–17]. The delay margin is defined as the maximum time delay that the system can withstand without losing stability. In the published research work, two approaches are used to determine the delay margin. The first one is based on Lyapunov–Krasovskii theorem and the second approach is based on tracking the eigenvalues in the s-domain. The s-domain methods proved to give less conservative delay margins; however, they can only be applied to constant time delay.

The small-signal theorem is used in Reference [7] to study the stability of a power system with a time delay. The impacts of the time delay on the supervisory power system stabilizers have also been investigated. In the power system, to achieve a robust performance over wide range of operating conditions, the centralized control with wide area measurements is usually adopted. The remote signals are received by the corresponding power system stabilizer through the PMUs where the time delay is introduced [8,9]. In Reference [8], the authors reported the improvement of the performance of the power system with the remote signals and they also found that the time delay could lead to power system instability if it is not considered during the design. An H_∞ Smith predictor is implemented in Reference [9] to compensate for the time delay. The simulation is used in Reference [10] to study the impact of the constant and random time delay on the stability of the load frequency control (LFC) system. In References [11,12], a less conservative criterion for computing the delay margin is presented where the Lyapunov–Krasovskii functional is used along with the Wirtinger inequality and Jenson integral inequality to bound the derivative of the Lyapunov function. In Reference [13], the delay margin for single-area and multi-area LFC system is computed through solving a set of linear matrix inequalities (LMIs). The LMIs are derived through solving Lyapunov–Krasovskii functional, replacing the time delay terms with the Newton–Leibnitz formula and introducing free weighting matrices (FWMs). It is reported in References [14,15] that the number of decision variables are reduced compared to the number of decision variables in Reference [13], and this will lead to less conservative results for the delay margin. Yu and Tomsovic [16] applied a simple LMI stability criterion for calculating the delay margin; however, the results are very conservative. In Reference [17], an exact method for computing the delay margin is introduced. The transcendental equation is transformed to normal polynomial in $j\omega$. The analysis is carried out in the frequency domain without any approximations, which reduces the conservativeness of the results. The exponential terms are eliminated and the transcendental equation is converted to a frequency dependent equation where the number of frequencies that cross the imaginary access are finite. The published research work either focuses on stabilization of the power system with the presence of the time delay or computing the delay margin required for system stability.

In Reference [18], the impact of the time delay on the power system is investigated. The impact of the parameters on the stability is studied by investigating their effect on the eigenvalues loci where a single-machine-infinite-bus (SMIB) is used as a case study. Jia et al. [19] used the Rekasius substitution to transform the transcendental characteristic equation into a polynomial, then the Routh criterion is used to determine the delay margin. Additionally, the impacts of the exciter gain, the generator mechanical output, and the generator damping on the delay margin are investigated. The impacts of the time delay on the stability region are investigated in Reference [20] and it is found that the time delay reduces the stability region of the power system. A direct frequency domain method was introduced in Reference [21]. The transcendental characteristic equation is converted to polynomial. The positive real roots of this polynomial coincide with the imaginary roots of the original characteristic equation and a formula is used to calculate the delay margin. The delay margin calculation is carried out analytically, and if a change in the system structure or the system order occurs, then the polynomial coefficients needs to be recalculated, which is the main weakness of the method; however, it gives accurate results. In Reference [22], a method based on the Lyapunov–Krasovskii theorem is used to analyze the delay-dependent stability of the power system; however, the delay margin results are a little bit conservative. A linear matrix inequalities approach is used in Reference [23] to study the delay dependent stability of the power system. Three criteria are introduced to compute the delay margin. The criterion with the least number of free weighting matrices has the least conservative results. In Reference [24], the order of the time-delayed power system is reduced using Jordan standardization, Taylor separation, and Schur simplification. This, in turn, increases the efficiency and reduces the computations. In Reference [25], Rekasius substitution is used to transform the transcendental characteristic equation into normal polynomial and a single-machine-infinite-bus system equipped with an automatic voltage regulator (AVR) and a power system stabilizer (PSS) is chosen as a case study. The delay margin is calculated for different values of the PSS gain.

In this paper, we present a method for computing the delay margin for the power system. Relative to the methods reported in the literature, the proposed method has a simple structure and is easy to follow while giving accurate values of the delay margin, which is very important in practice. The rest of the paper is organized as follows: In the next section the general dynamic model of the power system with time delay is briefly described. Then, the stability criterion for determining the delay margin is introduced where the sweeping test and the binary iteration are used to compute the delay margin. A single-machine-infinite-bus system equipped with automatic voltage regulator and power system stabilizer is chosen as a case study. In the results section, the results of the delay margin computation using the proposed method are compared with the results of the most recent published research work. The main findings of the paper are summarized in the discussion section. The last section contains the conclusions drawn from this work.

2. Materials and Methods

The presented method is based on the analysis in the s-domain without any approximation. The dynamics of the power system is nonlinear, therefore the model of the power system should be linearized around its operating point. The dynamic of the power system with time delay can be described using the following [19–21]:

$$\begin{cases} \dot{x} = f(x, y, x_\tau, y_\tau, p) \\ 0 = g(x, y, p) \\ 0 = g(x_\tau, y_\tau, p) \end{cases} \tag{1}$$

where $x \in R^n$ is the states vector, $y \in R^m$ is the algebraic variables vector, $p \in R^p$ is the bifurcation variables vector, $x_\tau := x(t-\tau) \in R^n$ and $y_\tau := y(t-\tau) \in R^m$ are the delayed states vector and delayed algebraic variables vector, respectively. Linearizing the power system around an equilibrium point (x_0, y_0), then the following equation can be derived [19–21]:

$$\begin{cases} \Delta\dot{x} = A_0\Delta x + A_\tau\Delta x_\tau + B_0\Delta y + B_\tau\Delta y_\tau \\ 0 = C_0\Delta x + D_0\Delta y \\ 0 = C_\tau\Delta x_\tau + D_\tau\Delta y_\tau \end{cases} \tag{2}$$

where

$$A_0 = \left.\frac{\partial f}{\partial x}\right|_p,\ B_0 = \left.\frac{\partial f}{\partial y}\right|_p,\ C_0 = \left.\frac{\partial g}{\partial x}\right|_p,\ D_0 = \left.\frac{\partial g}{\partial y}\right|_p,\ A_\tau = \left.\frac{\partial f}{\partial x_\tau}\right|_p,\ B_0 = \left.\frac{\partial f}{\partial y}\right|_p,\ C_0 = \left.\frac{\partial g}{\partial x}\right|_p,\ D_\tau = \left.\frac{\partial g}{\partial y_\tau}\right|_p$$

Given that D_0 and D_τ are nonsingular, then Equation (2) can be simplified to [19–21]:

$$\Delta\dot{x}(t) = \widetilde{A}_0\Delta x(t) + \widetilde{A}_\tau\Delta x(t-\tau) \tag{3}$$

where

$$\widetilde{A}_i = A_i - B_i \cdot D_i^{-1} \cdot C_i,\ i = 0, \tau$$

Taking the Laplace transform of Equation (3), the stability of the delay-dependent power system stability is determined through solving the following characteristic equation:

$$\det(\lambda \cdot I - \widetilde{A}_0 - \widetilde{A}_\tau \cdot e^{-\tau\cdot\lambda}) = 0 \tag{4}$$

Equation (4) is a transcendental equation and has been the subject of research for many years. The system is asymptotically stable for a given delay if all the roots of Equation (4) lie in the left-half plane. The free delay system is assumed to be stable and all the roots are on the left-half plane.

For some value of the delay, one or more roots will cross the imaginary axis. One of the approaches is to replace s with $j\omega$ and perform the analysis in the frequency domain.

2.1. The Proposed Method

Time delay systems can be either delay independent or delay dependent. The delay-dependent system is asymptotically stable for $\tau < \tau_d$, marginally stable for $\tau = \tau_d$, and unstable for $\tau > \tau_d$. The delay-independent system is asymptotically stable for any positive value of the time delay. For the power system represented by Equation (3) to be asymptotically stable independent of delay, we must have:

$$\det(sI - \widetilde{A}_0 - \widetilde{A}_\tau e^{-s\tau}) \neq 0 \, \forall s \in C_+, \, \forall \tau \geq 0 \tag{5}$$

where C_+ is the open right-half plane. If Equation (5) is satisfied, then there are no positive roots for any value of the time delay. The linear system can be delay independent (see Figure 1a), where the roots of the system remain in the left-half plane for any time delay $\tau > 0$. The time delay dependent system may have only one delay margin as shown in Figure 1b, in this case when the time delay equals the delay margin, $\tau = \tau_d$, where one or more roots will cross the imaginary axis moving from the left-half plane to the right-half plane, resulting in system instability. The roots will remain in the right-half plane as the time delay is increased beyond the delay margin, $\tau > \tau_d$. In some cases, the system may have multiple delay margins as shown in Figure 1c. In this case, as the time delay increases, one or more roots will cross the imaginary axis at ω_{c1} when $\tau = \tau_{d1}$. If the time delay is increased to more than τ_{d1}, the roots move and stay in the right-half plane, and when the time delay equals τ_{d2}, the roots move back to the left-half plane and cross the imaginary axis at ω_{c2} and the system returns to stability again. When the time delay is increased to more than τ_{d3}, the roots will cross the imaginary axis at ω_{c3}. The roots will remain in the right-half plane as the time delay is increased and the system becomes unstable.

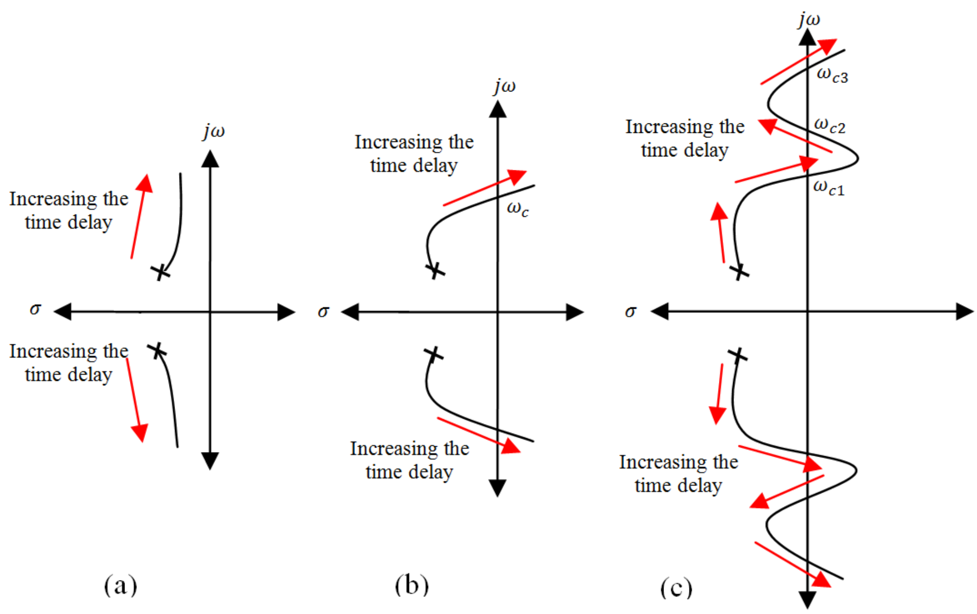

Figure 1. (**a**) A delay-independent system, (**b**) a delay-dependent system with a single delay margin, and (**c**) a delay-dependent system with multiple delay margins.

The delay-dependent stability implies that for time delays less than the delay margin, the system is asymptotically stable and all the roots are on the closed left-half plane, and when the time delay exceeds the delay margin, the system becomes unstable and some roots will be on the right-half plane. In this manner, the roots will cross the imaginary axis when $\tau = \tau_d$. We are interested in determining both the delay-independent and delay-dependent conditions of the system. To simplify the analysis, we replace s with $j\omega$. Now, we turn our attention to finding the delay that produce frequencies on the imaginary axis. Then Equation (3) is said to be asymptotically stable independent of delay if [26]:

$$\det(j\omega I - \widetilde{A}_0 - \widetilde{A}_\tau e^{-j\omega\tau}) \neq 0 \; \forall \omega \in (0, \infty), \; \tau \geq 0 \tag{6}$$

If Equation (6) is not satisfied for some values of ω, then the system is delay-dependent stable. Now the problem is to find the crossing frequency, ω_c, where the roots cross the imaginary axis. To find the crossing frequencies, we use the spectral radius in the following definition.

Definition 1 [27]**.**
The spectral radius of a two-matrices pair is defined as:

$$\underline{\rho}(\widetilde{A}_0, \widetilde{A}_\tau) := \min\left\{ |\lambda| \middle| \det(\widetilde{A}_0 - \lambda \widetilde{A}_\tau) = 0 \right\} \tag{7}$$

where $\lambda_i(\widetilde{A}_0)$ is the ith eigenvalue of the matrix $\widetilde{A}_0$ *and* $\lambda_i(\widetilde{A}_0, \widetilde{A}_\tau)$ is the generalized eigenvalue of matrix pair $\widetilde{A}_0$, and $\widetilde{A}_\tau$.

The computation of the delay margin is carried out in the ω domain. To compute the maximum delay margin we adopt the sweeping test [28]. The sweeping test is very valuable tool especially with the advances in the computing capabilities of the today's computers. The seeping test is better for its simplicity with less computation and accurate results. To find the delay margin of the power system we use the following theorem.

Theorem 1 [27]**.**
For Equation (3) stable at τ_d = *0*, i.e., $\widetilde{A}_0$ + $\widetilde{A}_\tau$ is stable and rank ($\widetilde{A}_\tau$) = *q*, we define:

$$\overline{\tau}_i := \begin{cases} \min\limits_{1 \leq k \leq n} \dfrac{\theta_k^i}{\omega_k^i}, & if\ \lambda_i(j\omega_k^i I - \widetilde{A}_0, \widetilde{A}_\tau) = e^{-j\theta_k^i} \\ & for\ some\ \omega_k^i \in (0, \infty), \theta_k^i \in [0, 2\pi] \\ \infty, & \underline{\rho}(j\omega I - \widetilde{A}_0, \widetilde{A}_\tau) > 1 \; \forall \omega \in (0, \infty) \end{cases}$$

Then $\tau_d := \min_{1 \leq i \leq q} \overline{\tau}_i$, and Equation (3) is stable for all $\tau \in [0, \tau_d)$ and becomes unstable at $\tau = \tau_d$.

Proof [26–29]**:**
Equation (3) is stable independent of the time delay if the following condition is satisfied:

$$\underline{\rho}(j\omega I - \widetilde{A}_0, \widetilde{A}_\tau) = \underline{\rho}(j\omega I - \widetilde{A}_0, \widetilde{A}_\tau e^{-j\omega\tau}) > 1 \text{ for } \omega > 0, \tau \geq 0 \tag{8}$$

Condition (8) implies that the system is stable with $\tau = 0$, that is, $\det(\widetilde{A}_0 + \widetilde{A}_\tau) \neq 0$. Now we assume that the system becomes unstable for some value of τ. This means $\tau_d < \infty$. Now, we assume that:

$$\det(j\omega I - \widetilde{A}_0 - \widetilde{A}_\tau e^{-j\omega\tau}) \neq 0, \; \forall \omega \in (0, \infty) \tag{9}$$

This can be true for $\omega \neq \omega_k^i$, and consequently at this condition:

$$\left| \lambda_i(j\omega I - \widetilde{A}_0, \widetilde{A}_\tau) \right| \neq 1 \; i = 1, \ldots, n \tag{10}$$

For any $\tau \in [0, \tau_d)$, $\tau\omega_k^i \neq \theta_k^i$ we must have:

$$\det(j\omega_k^i I - \widetilde{A}_0 - \widetilde{A}_\tau e^{-j\omega_k^i \tau}) \neq 0 \quad (11)$$

When $\tau = \tau_d$ there is a pair (ω_k^i, θ_k^i) that satisfies $\tau_d = \theta_k^i / \omega_k^i$, and consequently:

$$\det(j\omega_k^i I - \widetilde{A}_0 - \widetilde{A}_\tau e^{-j\omega_k^i \tau_d}) = \det(j\omega_k^i I - \widetilde{A}_0 - \widetilde{A}_\tau e^{-j\theta_k^i}) = 0 \quad (12)$$

Corollary 1 [27]: Equation (3) is stable independent of delay if and only if:

(i) $\widetilde{A}_0$ is stable,
(ii) $\widetilde{A}_0 + \widetilde{A}_\tau$ is stable, and
(iii) $\underline{\rho}(j\omega I - \widetilde{A}_0, \widetilde{A}_\tau) > 1, \forall \omega > 0$

The three conditions in Corollary 1 represent the delay-independent stability, where (i) states that the system is stable at $\tau = 0$, (ii) states the system is stable at $\tau = \infty$, and (iii) states the system is stable for every τ in the range $\tau \in [0, \infty)$.

Theorem 1 determines both the delay-independent and the delay-dependent stability. First, we can verify the delay-independent stability by checking the following condition:

$$\underline{\rho}(j\omega I - \widetilde{A}_0, \widetilde{A}_\tau) > 1 \ \forall \omega \in (0, \infty)$$

If the above condition is satisfied, then the system is stable independent of time delay, and if it is not satisfied for some values of ω that makes $\underline{\rho}(j\omega I - \widetilde{A}_0, \widetilde{A}_\tau) < 1$, then we calculate the crossing frequencies and the corresponding delay margin.

2.2. The Single-Machine-Infinite-Bus Power System with AVR and PSS

A single machine infinite bus system with AVR and PSS is shown in Figure 2 and the block diagram of the system is shown in Figure 3 [25,30,31]. The time delay is present in the terminal voltage measurement. For the stability analysis, the linear model is usually used. The flux-decay model with an exciter is shown in Figure 4 [25,30,31]. PSSs are used in power systems to dampen the inherent oscillations and improve the stability. The PSS signal is fed to the AVR to regulate the terminal voltage of the generator. The basic block diagram of a PSS is shown in Figure 5 [25,30,31]. The generator speed deviation is the input signal of the PSS. The PSS contains gain, K_{PSS}, washout block, and a lead-lag compensator. The washout is a high-pass filter and the lead-lag block compensates the phase lag between the exciter input and the electrical torque of the generator [30].

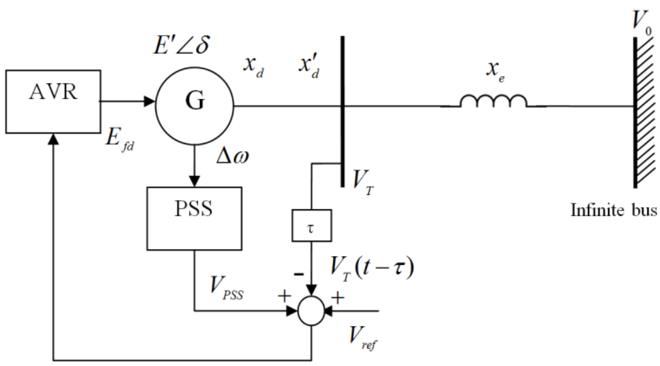

Figure 2. A single-machine-infinite-bus power system with an exciter.

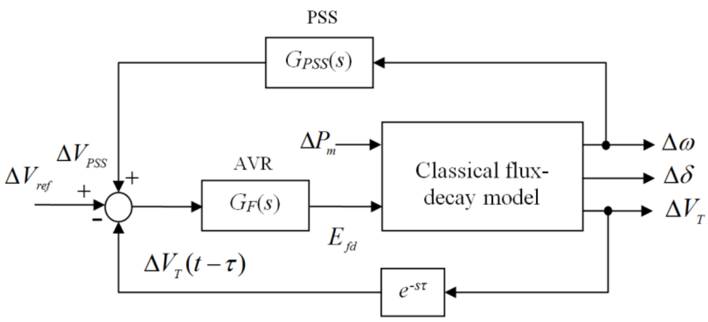

Figure 3. The block diagram of a single-machine-infinite-bus power system with AVR and PSS.

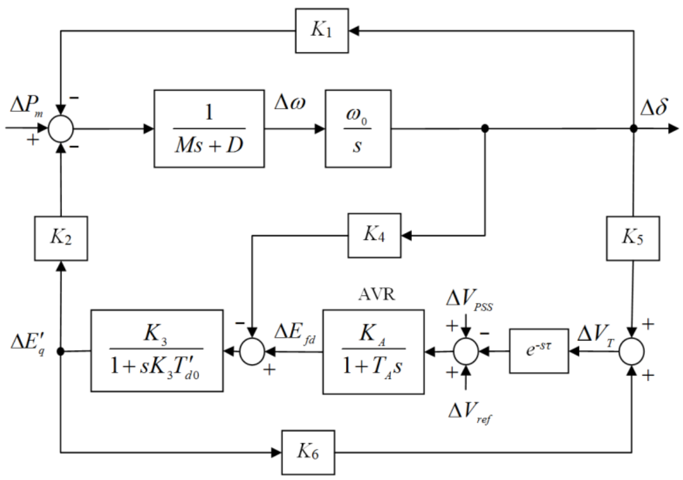

Figure 4. The model of the SMIB system with AVR and communication delay.

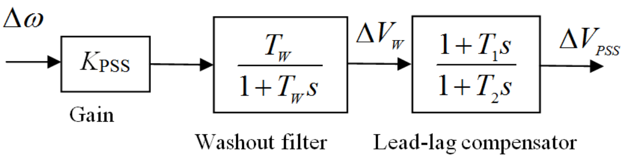

Figure 5. The block diagram of the power system stabilizer.

The SMIB system with AVR and PSS can be expressed as Equation (3) where;

$$\Delta x(t) = \begin{bmatrix} \Delta\delta & \Delta\omega & \Delta E'_q & \Delta E_{fd} & \Delta V_\omega & \Delta V_{PSS} \end{bmatrix}^T$$

$$\widetilde{A}_0 = \begin{bmatrix} 0 & \omega_0 & 0 & 0 & 0 & 0 \\ -\frac{K_1}{M} & -\frac{D}{M} & -\frac{K_2}{M} & 0 & 0 & 0 \\ -\frac{K_4}{T'_{d0}} & 0 & -\frac{1}{K_3T'_{d0}} & \frac{1}{T'_{d0}} & 0 & 0 \\ 0 & 0 & 0 & -\frac{1}{T_A} & 0 & \frac{K_A}{T_A} \\ -\frac{K_{PSS}K_1}{M} & -\frac{K_{PSS}D}{M} & -\frac{K_{PSS}K_2}{M} & 0 & -\frac{1}{T_\omega} & 0 \\ -\frac{K_{PSS}K_1T_1}{MT_2} & -\frac{K_{PSS}DT_1}{MT_2} & -\frac{K_{PSS}K_2T_1}{MT_2} & 0 & \left(\frac{1}{T_2} - \frac{T_1}{T_2T_\omega}\right) & -\frac{1}{T_2} \end{bmatrix}$$

$$\widetilde{A}_\tau = \begin{bmatrix} 0 & 0 & 0 & 0 & 0 & 0 \\ 0 & 0 & 0 & 0 & 0 & 0 \\ 0 & 0 & 0 & 0 & 0 & 0 \\ -\frac{K_5K_A}{T_A} & 0 & -\frac{K_6K_A}{T_A} & 0 & 0 & 0 \\ 0 & 0 & 0 & 0 & 0 & 0 \\ 0 & 0 & 0 & 0 & 0 & 0 \end{bmatrix}$$

The parameters in the model are defined as [25,30,31]:
The SMIB with an exciter:

δ	The generator angle
ω	The generator speed with ω_B the base speed
E'_q	The generator voltage behind the transient reactance
E_{fd}	The exciter output voltage, and E_{fd0} is the reference
K_A, T_A	The time constant and the gain of the exciter
P_m	The mechanical power
D	The generator damping factor
M	The moment of inertia
T'_{d0}	The open-loop time constant of the armature winding
V_0	The infinite bus voltage
V_T	The generator terminal voltage
x_e	The transmission line reactance
x'_d	The transient reactance
x_d	The synchronous reactance
T_1, T_2	The time constants of the Lead-lag compensator
T_w	The time constant of the washout filter
K_{PSS}	The gain of the power system stabilizer

The constants K_1–K_6 are given in Appendix A. K_1–K_6 can be determined using the initial conditions through solving the following set of equations. Linearizing Equation (1) around the operating point and using a number of simplifications, the Heffron–Phillips Model can be derived [32–34].

3. Results

The parameters of the SMIB system with AVR and PSS are given in Table 1.

Table 1. The parameters of the single-machine-infinite-bus power system [35].

M	D	x_d	x'_d	T'_{d0}	x_e
6.4	0.0	2.5	0.39	9.6	0.5
x_q	V_t	K_{PSS}	V_∞	ω_0	r_s
2.1	$1.0\angle 15$	5	1.05	377.0	0.0
r_e	T_1	T_2	T_W	K_A	T_A
0.0	0.5	0.1	2.0	100	0.05

To find the delay margin, we used Theorem 1 and the following algorithm:

Step 1: With the system parameters, compute $\widetilde{A}_0$ and $\widetilde{A}_\tau$. Using the sweep test, check if the system is stable independent of delay, that is $\underline{\rho}(j\omega I - \widetilde{A}_0,) > 1$ for $\omega \in (0, \infty)$. If for some values of ω, $\underline{\rho}(j\omega I - \widetilde{A}_0, \widetilde{A}_\tau) = 1$, then proceed to step 2; else the system is stable independent of the time delay.

Step 2: Define a range $\omega \in [\omega_1, \omega_2]$. At ω_1 the spectral radius $\underline{\rho}(j\omega I - \widetilde{A}_0, \widetilde{A}_\tau) < 1$ and at ω_2 the spectral radius $\underline{\rho}(j\omega I - \widetilde{A}_0, \widetilde{A}_\tau) > 1$. Now, $\omega_c \in [\omega_1, \omega_2]$.

Step 3: Use the binary iteration to find the crossing frequency with a given error tolerance ω_e. We set $\omega_{new} = (\omega_1 + \omega_2)/2$. If $\underline{\rho}(j\omega_{new} I - \widetilde{A}_0, \widetilde{A}_\tau) > 1$ then $\omega_2 = \omega_{new}$, and if $\underline{\rho}(j\omega_{new} I - \widetilde{A}_0, \widetilde{A}_\tau) < 1$ then $\omega_1 = \omega_{new}$. Now the search range is reduced until the desired accuracy is reached.

Step 4: When the desired accuracy is reached, we calculate θ_k^i through solving $\lambda_i(j\omega_k^i I - \widetilde{A}_0, \widetilde{A}_\tau) = e^{-j\theta_k^i}$. Finally, $\tau_d = \min\limits_{1 \le k \le n} (\theta_k^i / \omega_k^i)$ is the desired delay margin.

The procedure for calculating the constants is given in Appendix A and they were given as: K_1 = 0.9223, K_2 = 1.0737, K_3 = 0.2967, K_4 = 2.2655, K_5 = 0.0050, and K_6 = 0.3572. For computing the delay margin, the algorithm is given in Figure 6. With K_{PSS} = 5, the system linear model was given as:

$$\widetilde{A}_0 = \begin{bmatrix} 0 & 377 & 0 & 0 & 0 & 0 \\ -0.14411 & 0 & -0.16777 & 0 & 0 & 0 \\ -0.23599 & 0 & -0.35112 & 0.10417 & 0 & 0 \\ 0 & 0 & 0 & -20 & 0 & 2000 \\ -0.72055 & 0 & -0.83884 & 0 & -0.5 & 0 \\ -3.6027 & 0 & -4.1942 & 0 & 7.5 & -10 \end{bmatrix} \widetilde{A}_\tau = \begin{bmatrix} 0 & 0 & 0 & 0 & 0 & 0 \\ 0 & 0 & 0 & 0 & 0 & 0 \\ 0 & 0 & 0 & 0 & 0 & 0 \\ -10.005 & 0 & -714.41 & 0 & 0 & 0 \\ 0 & 0 & 0 & 0 & 0 & 0 \\ 0 & 0 & 0 & 0 & 0 & 0 \end{bmatrix}$$

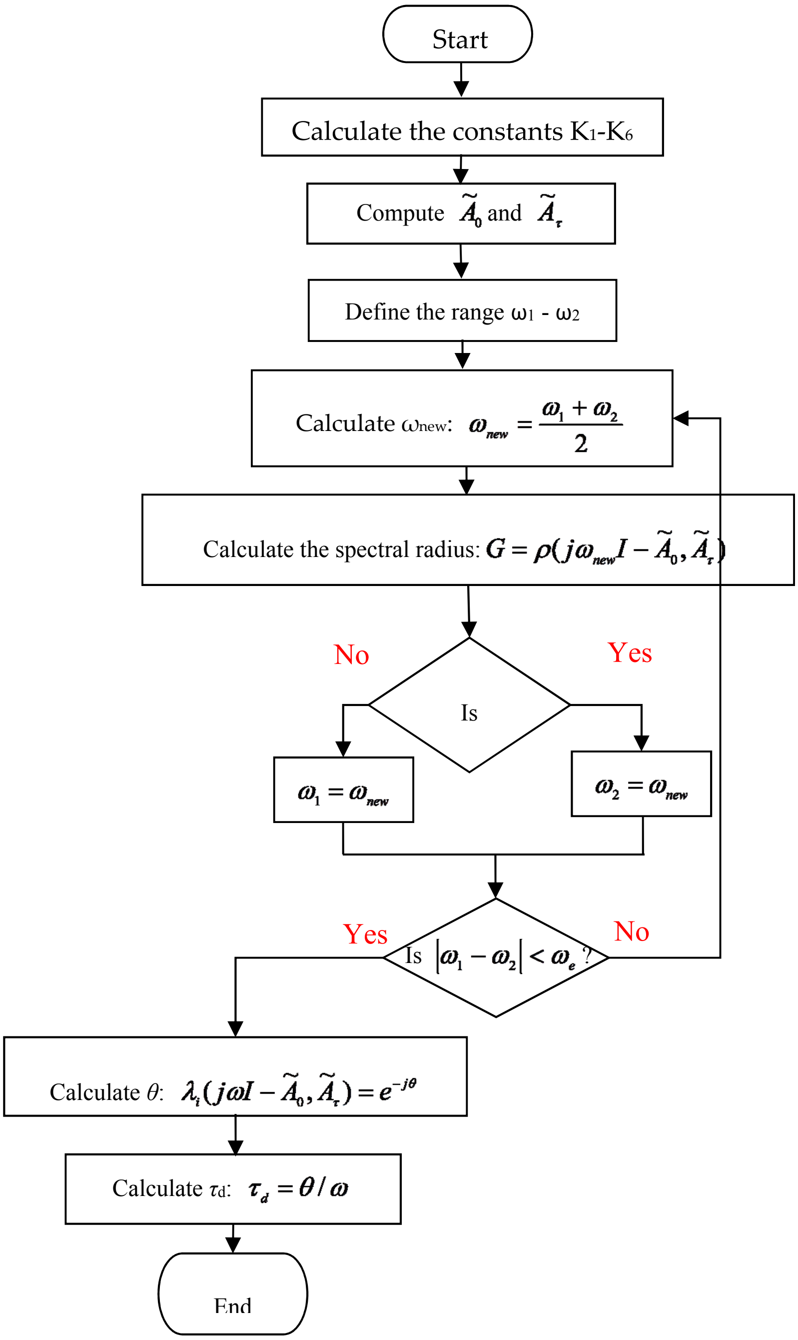

Figure 6. The delay margin computation algorithm.

Applying the algorithm, the crossing frequencies were given as: ω_{c1} = 2.8854, ω_{c2} = 8.8884, and ω_{c3} = 9.5856, which are shown in Figure 7. The corresponding crossing angles were: θ_{c1} = 1.2712, θ_{c2} = 2.8827, and θ_{c3} = 1.8194. The spectral radius as a function of the frequency is shown in Figure 7. This made the delay margins τ_1 = 0.44056 s, τ_2 = 0.32432 s, and τ_3 = 0.18981 s. The minimum delay margin was 0.18981 s, which was obtained with ω_{c3} = 9.5856 rad/s and θ_{c3} = 1.8194 rad. The terminal voltage with the different delay margins is shown in Figures 8–10.

Using the parameters in Reference [25], with K_{PSS} = 20, the constant parameters K_1–K_6 were given as K_1 = 1.0058, K_2 = 0.8441, K_3 = 0.36, K_4 = 1.0805, K_5 = 0.0468, and K_6 = 0.4991. With the proposed method, the crossing frequencies were ω_{c1} = 2.5141 rad/s, ω_{c2} = 11.0472 rad/s, and ω_{c3} = 13.1185 rad/s, and the corresponding crossing angles were θ_{c1} = 1.2465 rad, θ_{c2} = 2.6160 rad, and θ_{c3} = 1.0310 rad. Therefore, the delay margins were τ_1 = 0.4958 s, τ_2 = 0.3320 s, and τ_3 = 0.0786 s. The spectral radius as a function of the frequency is shown in Figure 11. The results of the proposed method and the method reported in Reference [25] are shown in Table 2. The terminal voltage with the different delay margins is shown in Figures 12–14. The delay margin with different PSS gains is shown in Table 3 along with the results of Reference [25]. The results of the proposed method are the same results reported in Reference [25]; however, for K_{PSS} = 0, the proposed method gave less conservative results. The terminal voltage with K_{PSS} = 0 and different time delays is shown in Figure 15.

Table 2. The delay margins and the corresponding crossing frequencies with the proposed method and the method in [25].

The parameter	Method	1	2	3
ω_c (rad/s)	The proposed method	2.5141	11.0472	13.1185
	The method in Ref. [25]	2.5140	11.0473	13.1187
τ (s)	The proposed method	0.4958	0.3320	0.0786
	The method in Ref. [25]	0.4958	0.3320	0.0786

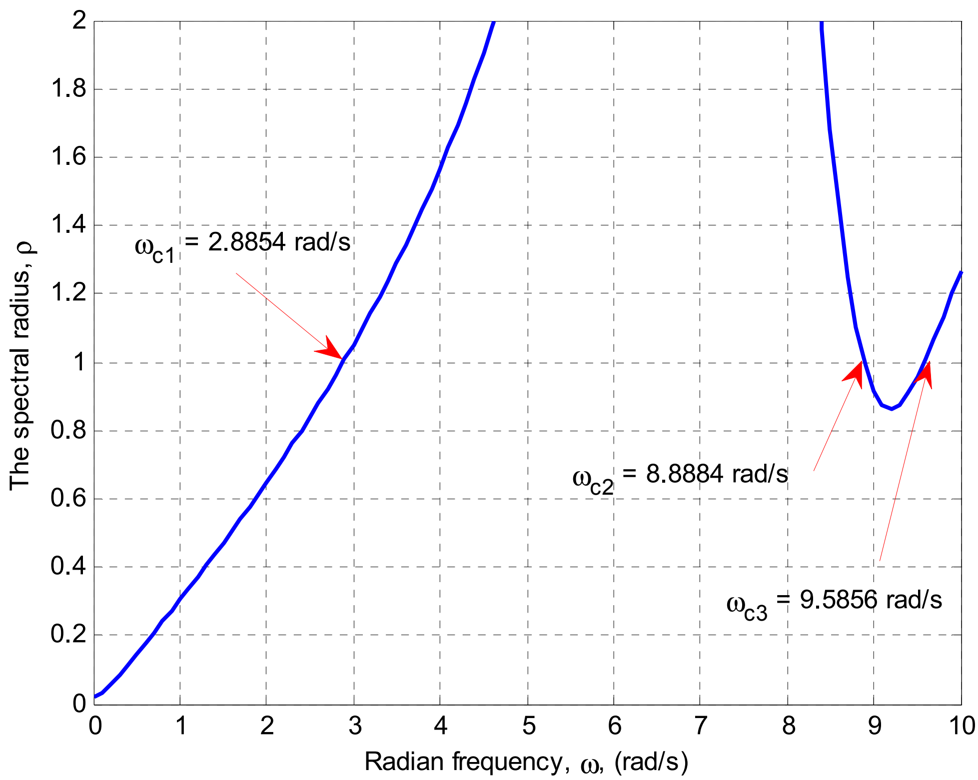

Figure 7. The spectral radius as function of ω.

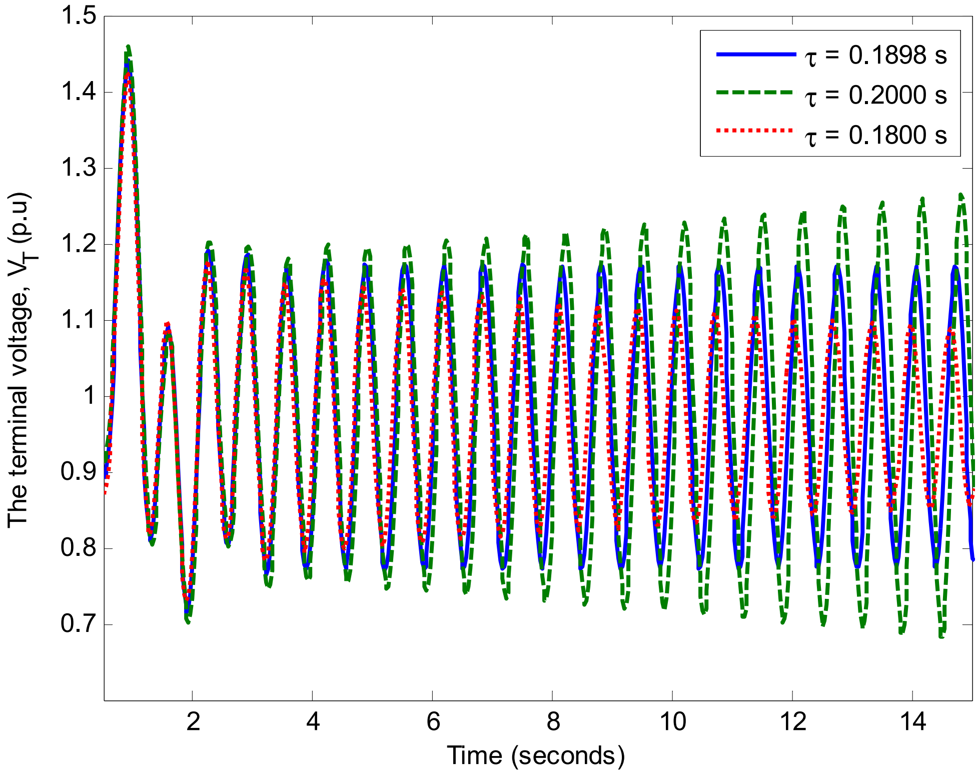

Figure 8. The terminal voltage with different time delays.

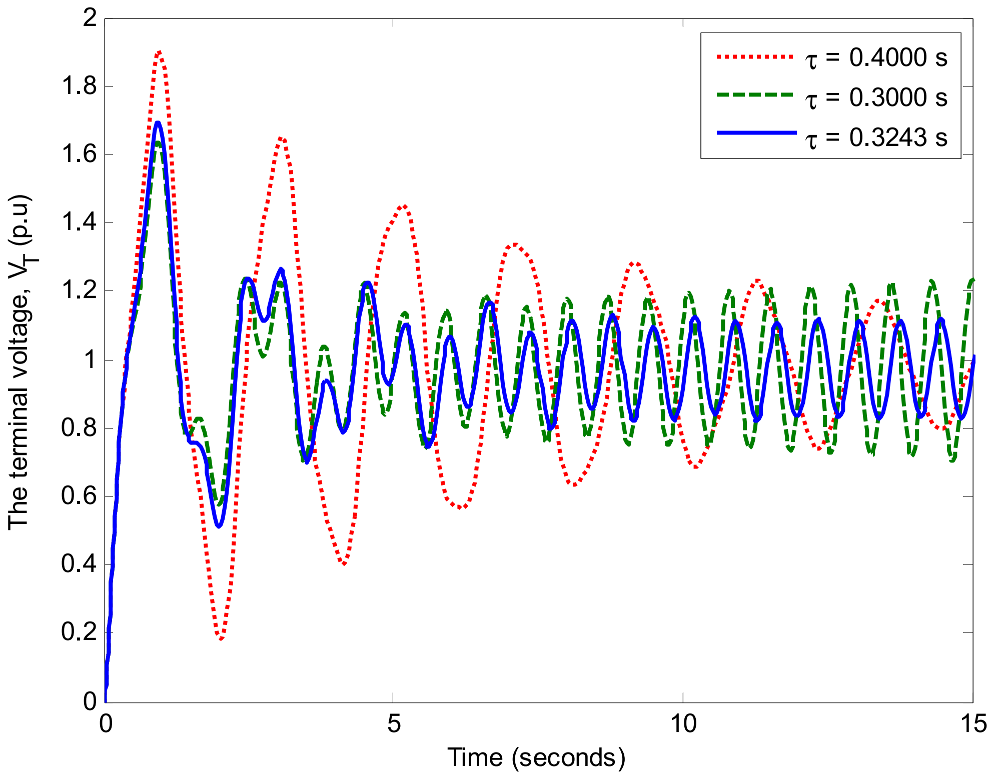

Figure 9. The terminal voltage with different time delays.

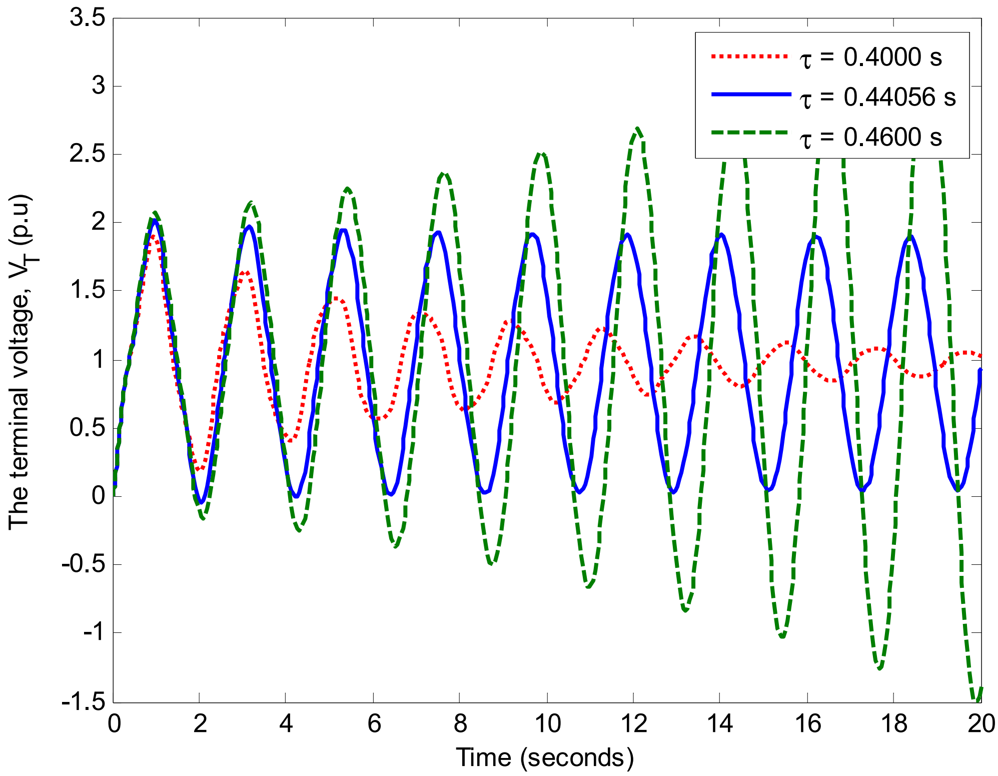

Figure 10. The terminal voltage with different time delays.

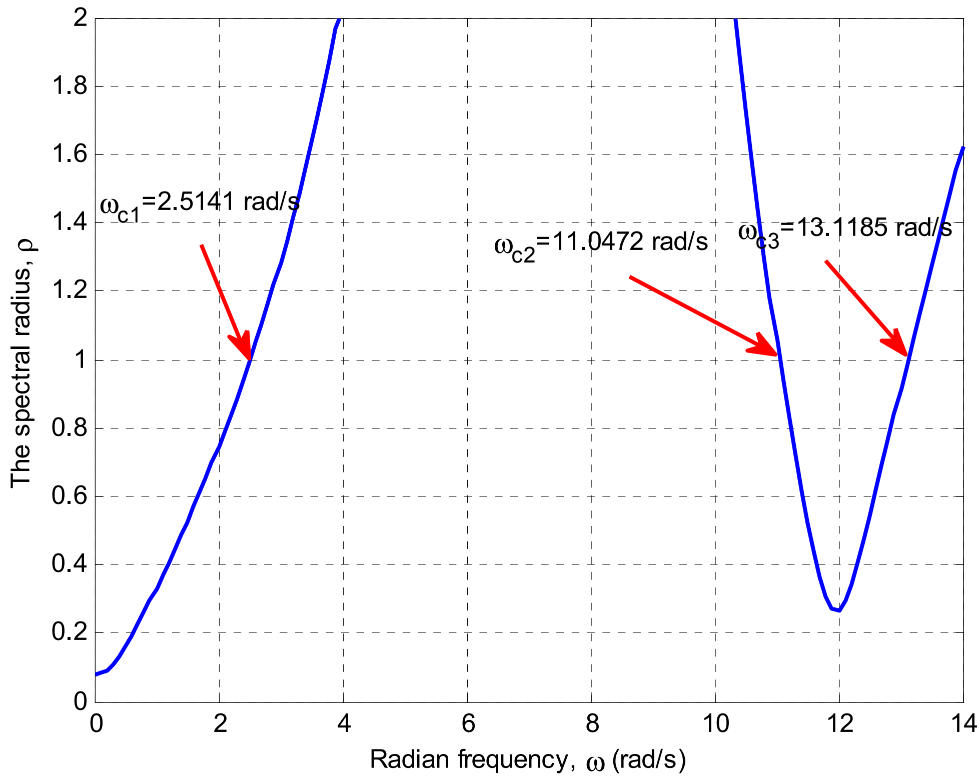

Figure 11. The spectral radius as function of ω.

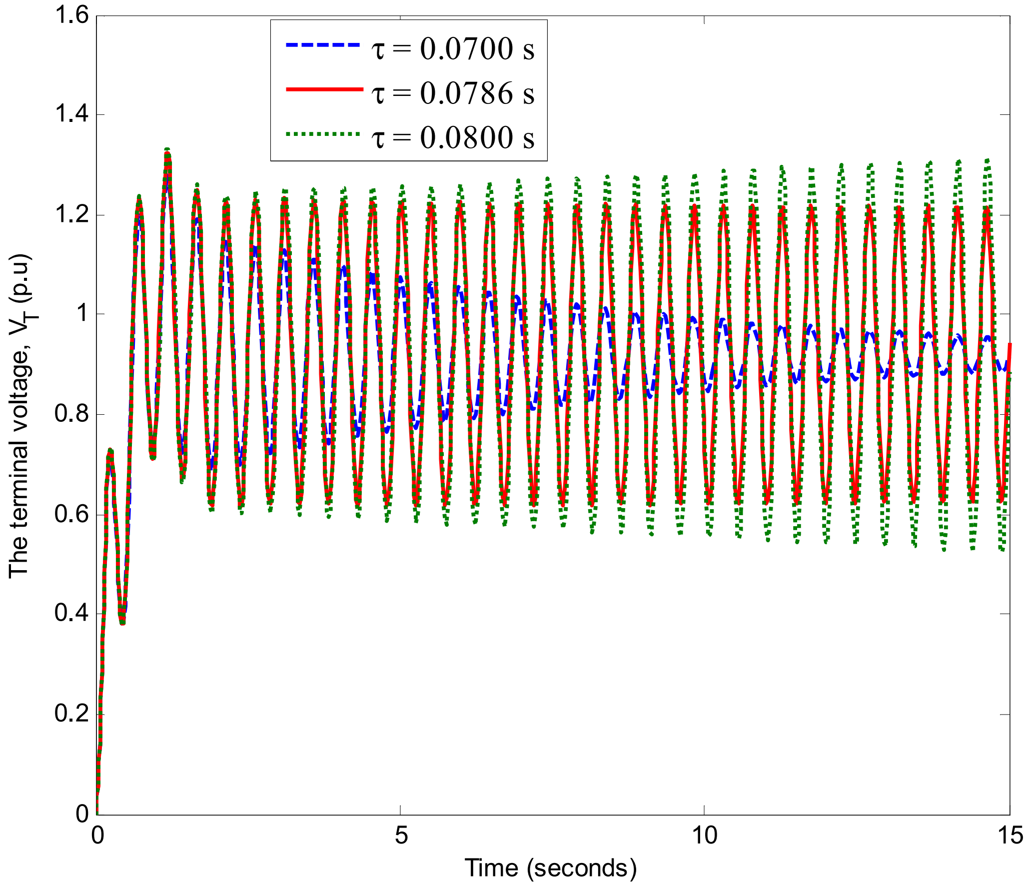

Figure 12. The terminal voltage with different time delays.

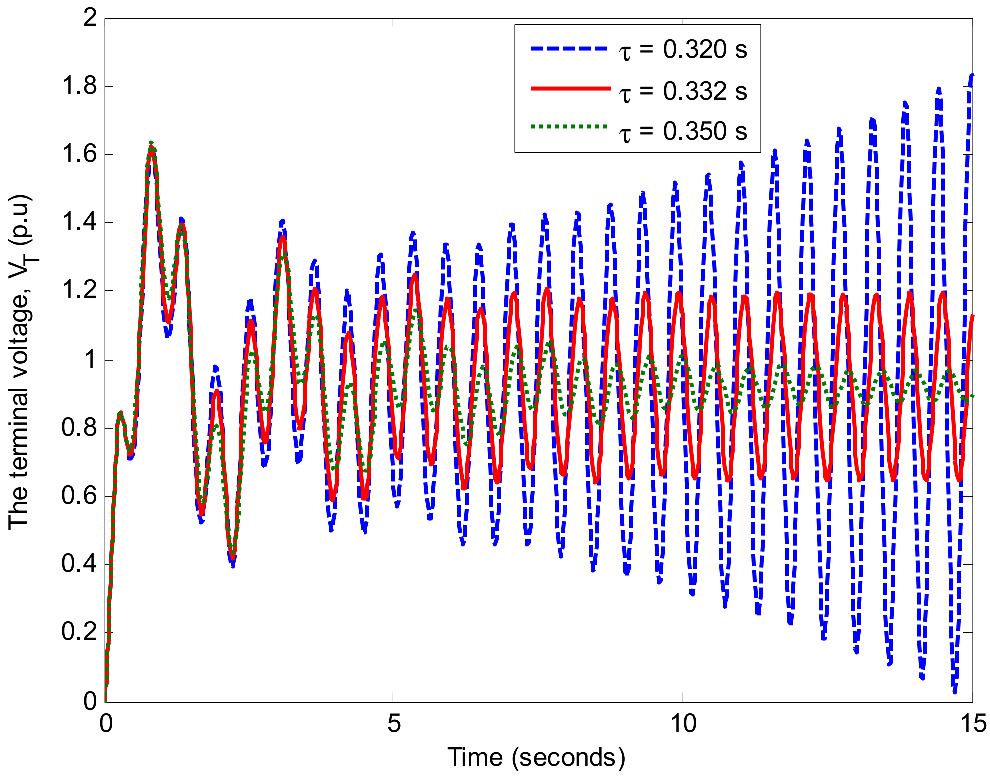

Figure 13. The terminal voltage with different time delays.

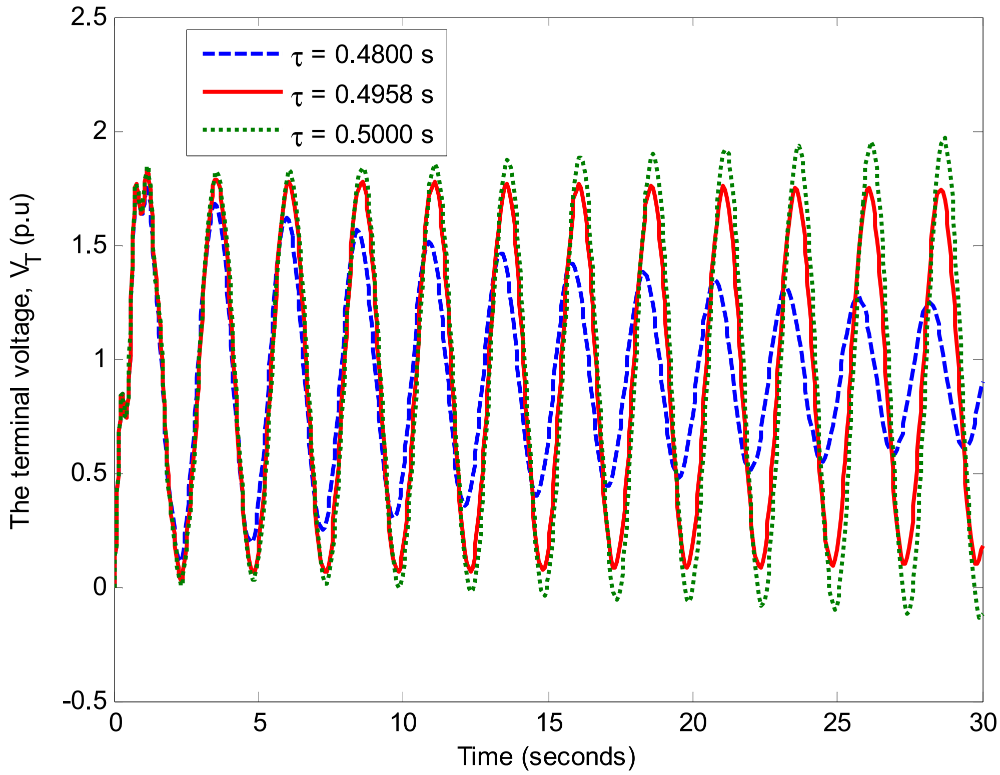

Figure 14. The terminal voltage with different time delays.

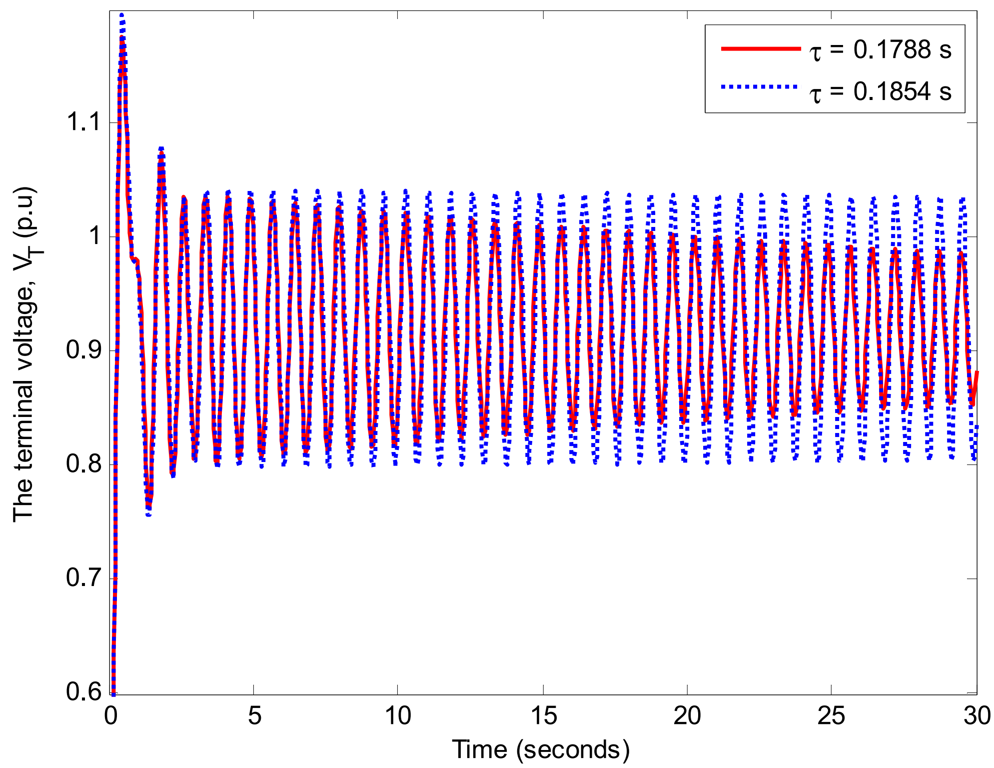

Figure 15. The terminal voltage with different time delays.

Table 3. The delay margin with different values of the PSS gain, K_{PSS}.

	Method	τ_1 (s)	τ_2 (s)	τ_3 (s)
K_{PSS} = 0	The proposed method	0.1854	0.4635	0.3984
	The method in Ref. [25]	0.1788	0.4579	0.3678
K_{PSS} = 5	The proposed method	0.1632	0.3774	0.4262
	The method in Ref. [25]	0.1632	0.3774	0.4262
K_{PSS} = 10	The proposed method	0.1289	0.3539	0.4508
	The method in Ref. [25]	0.1289	0.3539	0.4508
K_{PSS} = 15	The proposed method	0.1010	0.3407	0.4738
	The method in Ref. [25]	0.1010	0.3407	0.4738
K_{PSS} = 20	The proposed method	0.0786	0.3320	0.4958
	The method in Ref. [25]	0.0786	0.3320	0.4958
K_{PSS} = 25	The proposed method	0.0600	0.3258	0.5171
	The method in Ref. [25]	0.0600	0.3258	0.5171
K_{PSS} = 30	The proposed method	0.0439	0.3214	0.5378
	The method in Ref. [25]	0.0439	0.3214	0.5378

The terminal voltages with K_{PSS} = 5 and different time delays are shown in the Figures 16–22. The behavior of the system can be explained as follows (see Figure 23): As the time delay increases, one or more roots will cross the imaginary axis and the system becomes unstable. If the time delay is increased further, the roots will cross the imaginary axis from the opposite side and the system returns to being stable again. As the time delay is increased, the roots will cross the imaginary axis and the system will become unstable as long as $\tau > \tau_3$. The spectral radius as a function of the radian frequency with different values of the PSS gain is shown in Figure 23.

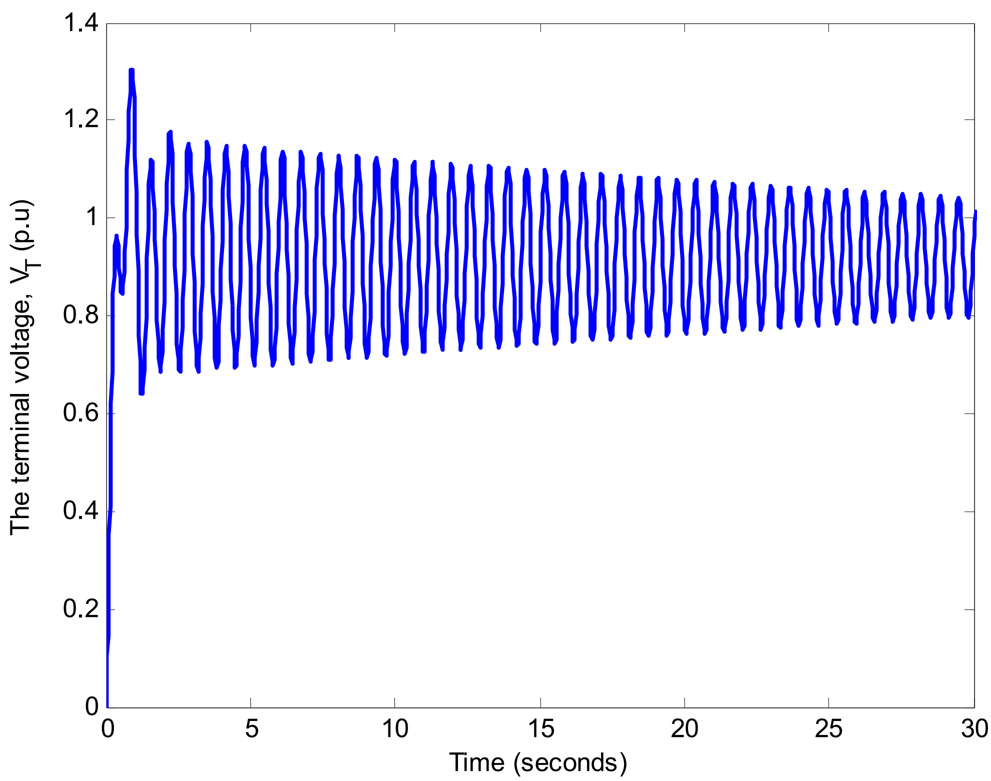

Figure 16. The terminal voltage with a 0.16 s time delay.

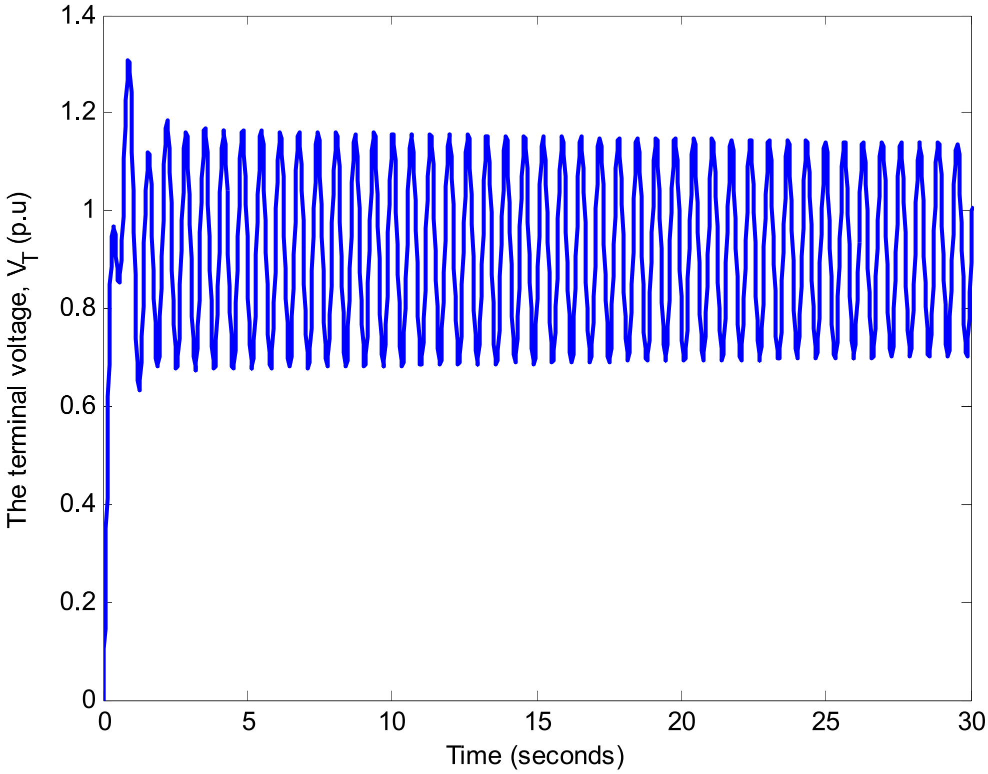

Figure 17. The terminal voltage with a 0.1632 s time delay.

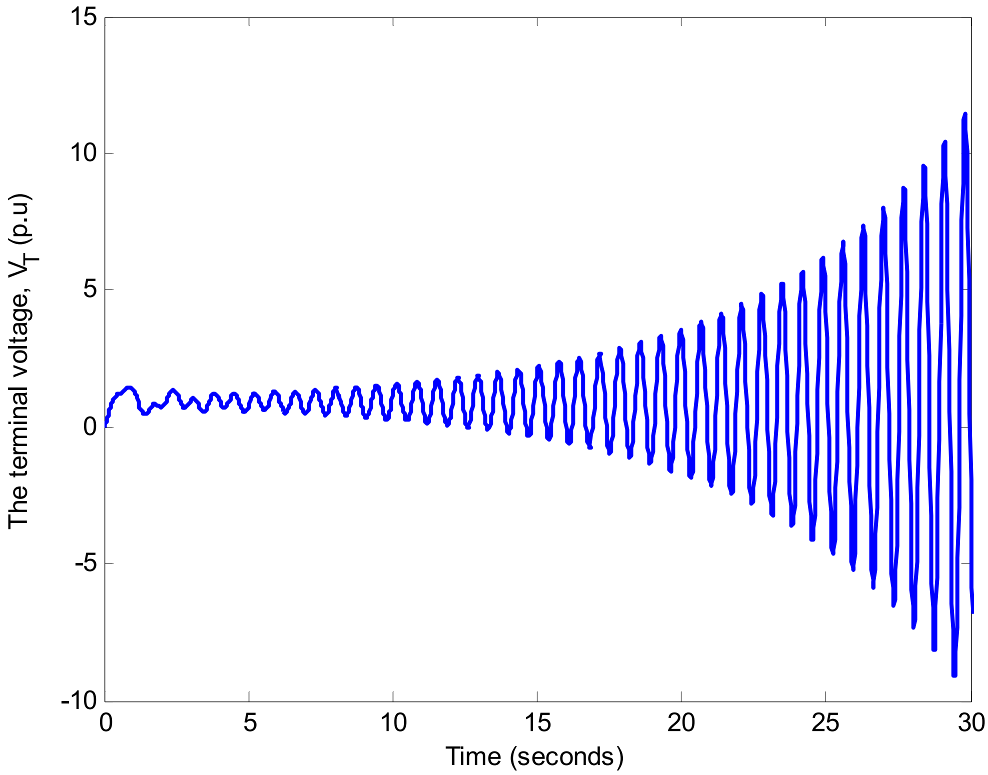

Figure 18. The terminal voltage with a 0.3 s time delay.

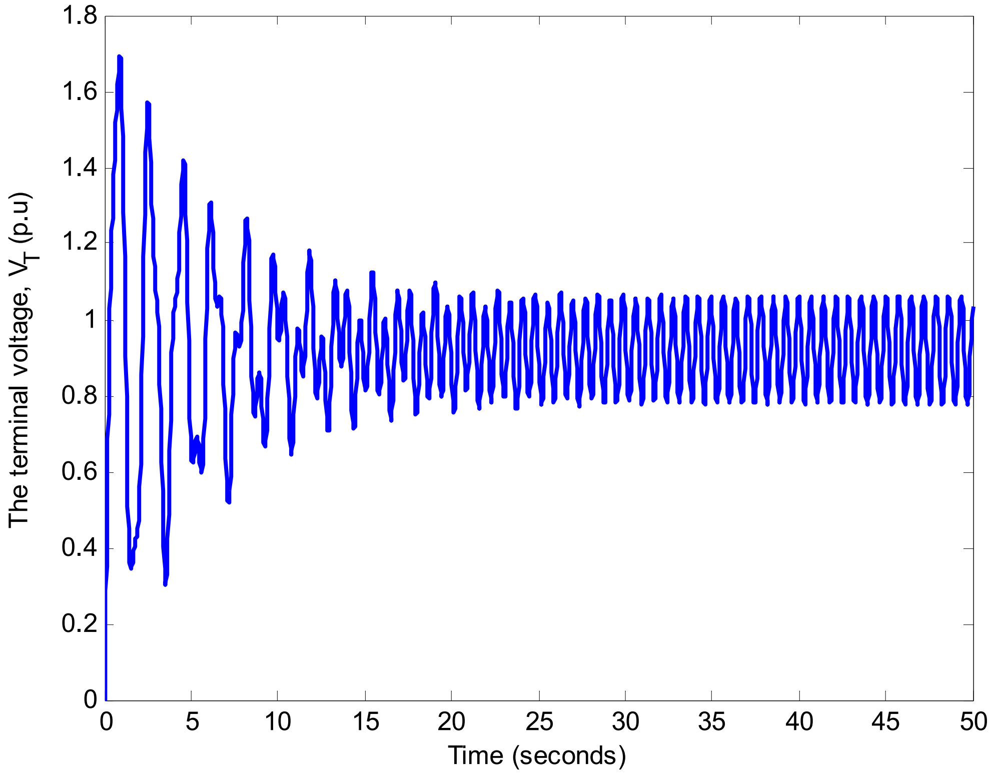

Figure 19. The terminal voltage with a 0.3744 s time delay.

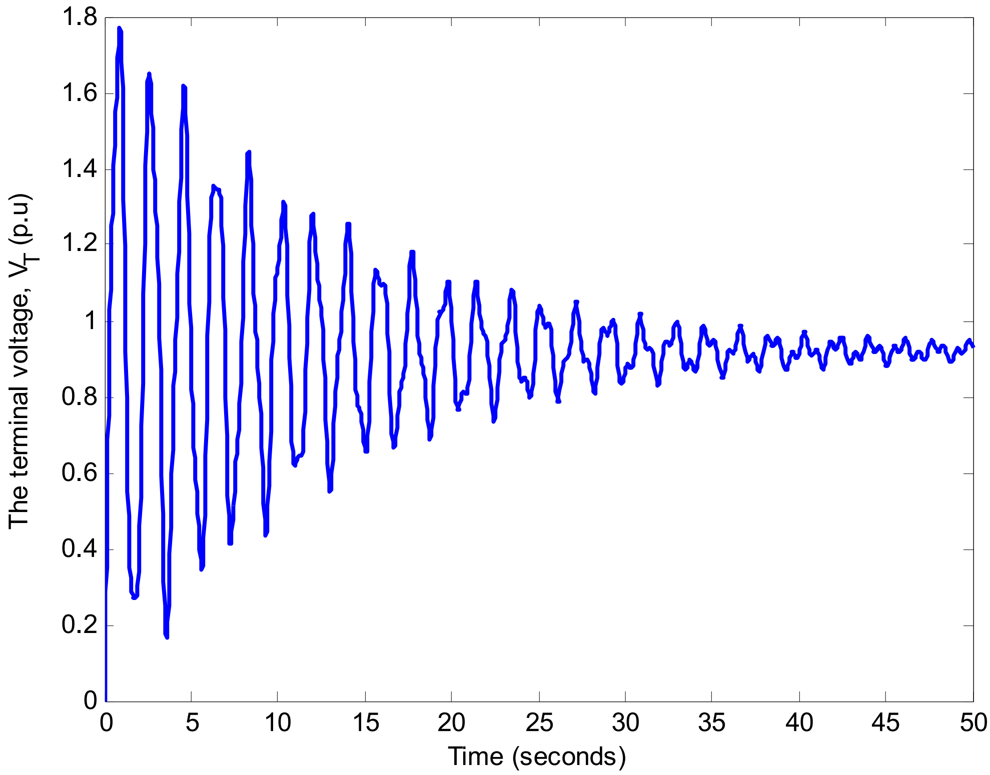

Figure 20. The terminal voltage with a 0.4 s time delay.

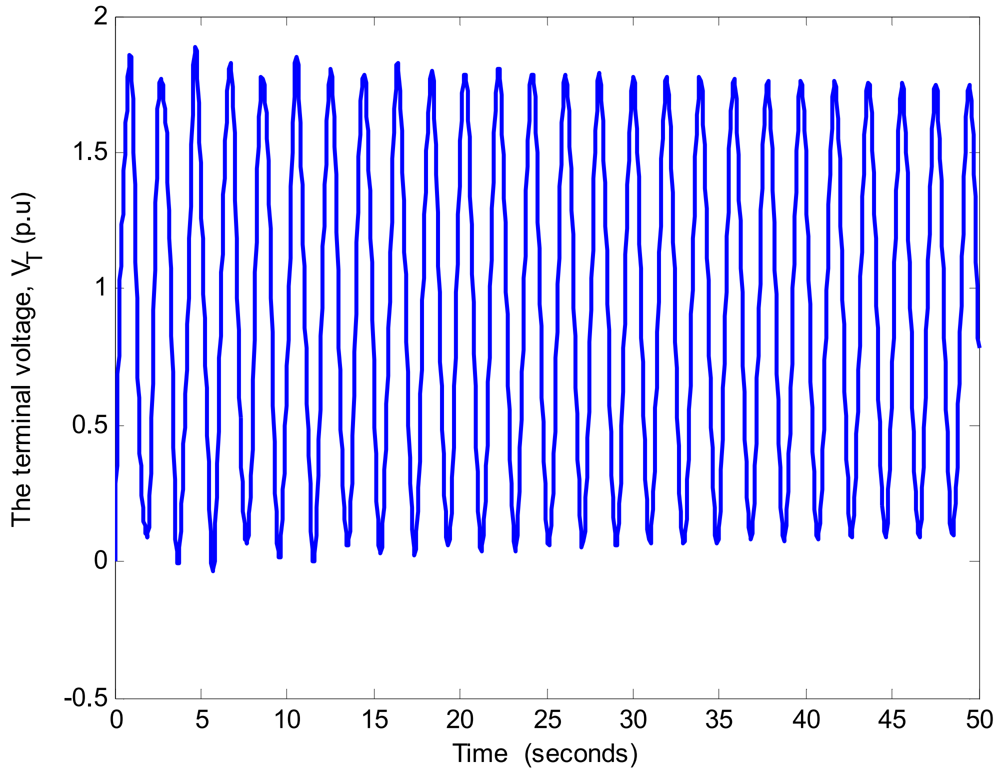

Figure 21. The terminal voltage with a 0.4262 s time delay.

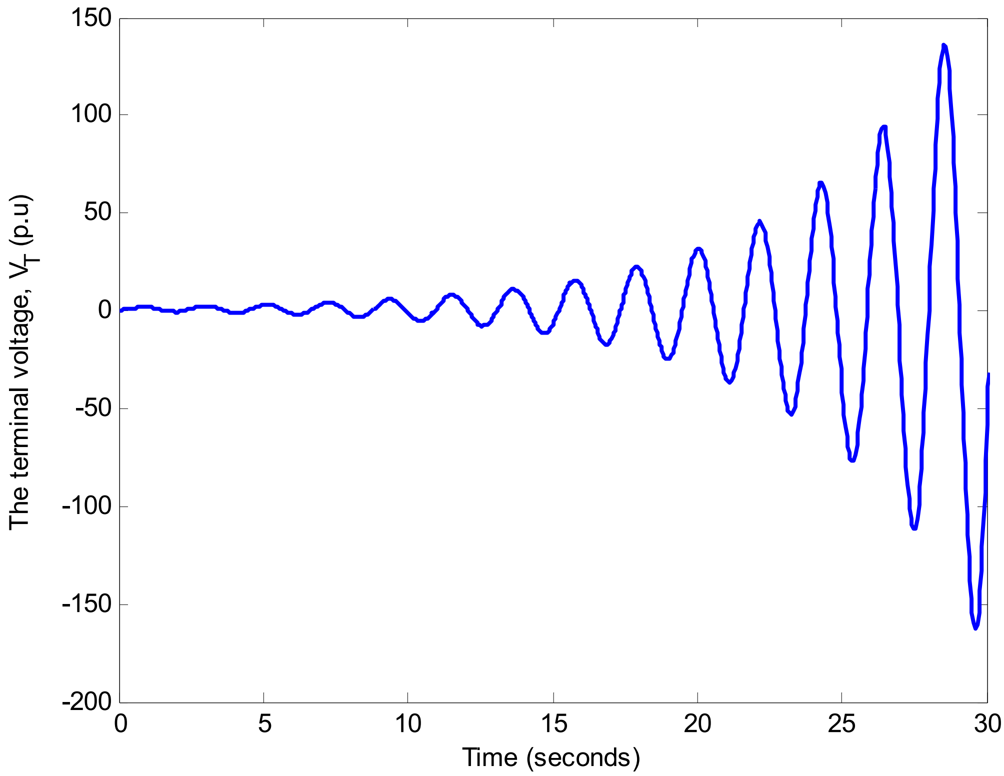

Figure 22. The terminal voltage with a 0.5 s time delay.

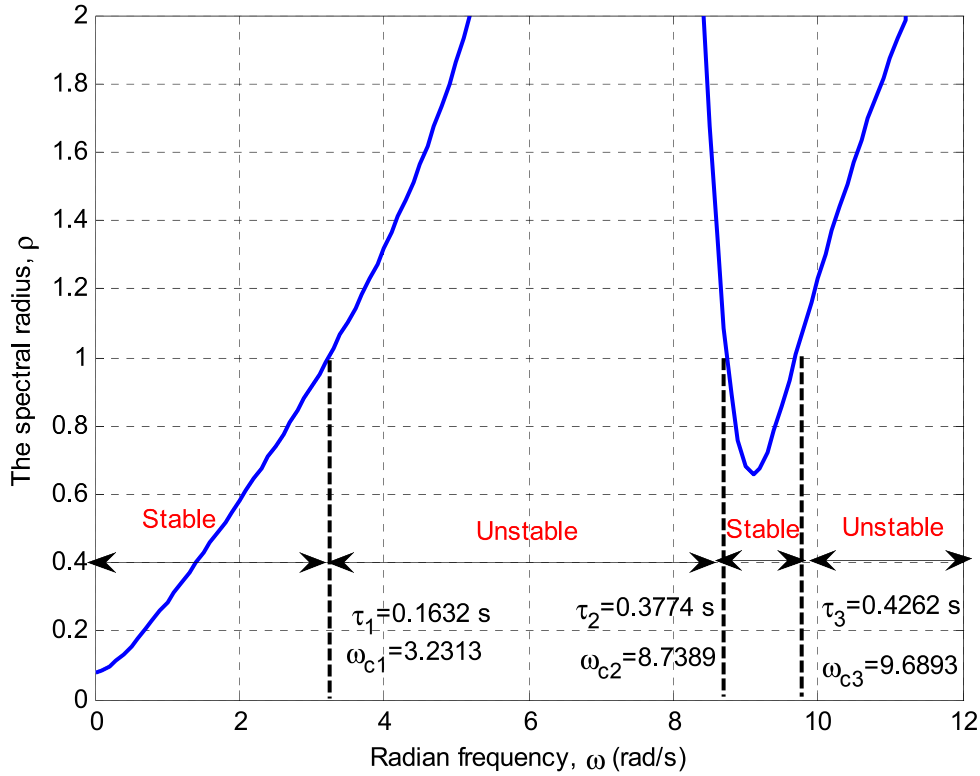

Figure 23. The spectral radius as function of ω.

4. Discussions

The presented methods in the literature are either less conservative and too complex to be implemented or simpler and more conservative. Using the sweeping test and the binary iteration algorithm, the method can accurately determine the maximum delay margin with fewer computations compared with the published methods in the literature. The method can be applied to analyze the stability of the power system or a general time-delay system. In this paper, the spectral radius is used to find the crossing frequencies, which leads to an exact calculation of the time-delay margin. For the single-machine-infinite-bus power system with AVR and PSS, increasing the PSS gain reduces the delay margin; this observation can be used in practice to aid in tuning the PSS gain to achieve the optimum performance. For the single-machine-infinite-bus power system with AVR and PSS, an interesting phenomenon has been observed. The system had multiple delay margins where three delay margins have been identified. The proposed method has two limitations. First, as the analysis in the s-domain, the method is only applicable to constant time delays. The method can be a useful tool for computing the delay margin and analyzing the stability of the power system with constant or bounded time delay. Second, the proposed method is applied to a single-delay, time-delay system and Theorem 1 cannot be applied for a time-delay system with multiple delays. In the case of multiple equal time delays, a similar theorem to Theorem 1 can be used; for more details the reader can refer to References [26–29].

5. Conclusions

In this paper, we proposed a method for computing the delay margin in a power system with a communication delay. The method is a frequency domain method without any approximation to the resultant delay system. The delay margins were computed through the binary iteration and the sweeping test. A single-machine-infinite-bus load power system has been chosen as case study and the delay margin values have been compared with values reported in the literature. The method gives accurate delay margins, which was proved using the time delay simulation and by comparison with the published methods. A single-machine-infinite-bus power system with AVR and PSS was used as a case study. The effect of the power system stabilizer gain on the delay margin has been investigated in the paper. The delay margin decreased with increasing power system stabilizer gain. The method is to be extended to analyze multi-time delays power system.

Author Contributions: A.K. derived the mathematical model and applied the stability criterion. A.S.P. made the simulations. A.K. and A.S.P. wrote and edited the paper.

Funding: This research received no external funding.

Conflicts of Interest: The authors declare no conflict of interest.

Nomenclature

δ	The generator angle
ω	The generator speed with ω_B the base speed
E'_q	The generator voltage behind the transient reactance
E_{fd}	The exciter output voltage, and E_{fd0} is the reference
K_A, T_A	The gain of the exciter and the time constant
$K_1 - K_6$	Constants
P_m	The mechanical power
D	The generator damping factor
M	The moment of inertia
T'_{d0}	The open-loop time constant of the armature winding
V_0	The infinite bus voltage
V_T	The generator terminal voltage
V_{PSS}	The Power System Stabilizer (PSS) signal
V_{ref}	The reference terminal voltage
V_w	The washout filter voltage
V_d	The direct axis voltage
V_q	The quadrature axis voltage
r_e	The transmission line resistance
r_s	The windings resistance
x_e	The transmission line reactance
x'_d	The transient reactance
x_d	The synchronous reactance
T_1, T_2	The time constants of the Lead-lag compensator
T_w	The time constant of the washout filter
K_{PSS}	The gain of the power system stabilizer
I_d	The direct axis current
I_q	The quadrature axis current

Appendix A

K_1–K_6 can be determined by the initial conditions through solving the following set of equations:

$$I_G e^{j\gamma} = \frac{\overline{V}_t - \overline{V}_\infty}{jx_e} \tag{A1}$$

$$E_0 \angle \delta_0 = \overline{V}_t + (r_s + jx_q) I_G e^{j\gamma} \tag{A2}$$

$$I_d + jI_q = I_G e^{j\gamma} e^{-j(\delta_0 - \pi/2)} \tag{A3}$$

$$V_d + jV_q = \overline{V}_t e^{-j(\delta_0 - \pi/2)} \tag{A4}$$

$$E_q = V_q + x'_d I_d \tag{A5}$$

$$E_{fd} = E_q + (x_d - x'_d) I_d \tag{A6}$$

$$E_{ref} = V_t + \frac{E_{fd}}{K_A} \tag{A7}$$

$$T_m = E_q I_q + (x_q - x'_d) I_d I_q \tag{A8}$$

The constants K_1–K_6 are given as:

$$\Delta = r_e^2 + (x_e + x_q)(x_e + x'_d) \tag{A9}$$

$$K_1 = -\tfrac{1}{\Delta}[I_q V_\infty (x'_d - x_q)\{(x_q + x_e)\sin\delta_0 - r_e \cos\delta_0\} + V_\infty\{(x'_d - x_q)I_d - E_q\}\{(x'_d + x_e)\cos\delta_0 + r_e \sin\delta_0] \tag{A10}$$

$$K_2 = \frac{1}{\Delta}[I_q \Delta - (x'_d - x_q)(x_q + x_e)I_q - r_e(x'_d - x_q)I_d + r_e E_q] \tag{A11}$$

$$K_3 = [1 + (x_d - x'_d)(x_q + x_e)/\Delta]^{-1} \tag{A12}$$

$$K_4 = \frac{V_\infty(x_d - x'_d)}{\Delta}[(x_q + x_e)\sin\delta_0 - r_e \cos\delta_0] \tag{A13}$$

$$K_5 = \frac{1}{\Delta}\left\{\frac{V_d}{V_t} x_q [r_e V_\infty \sin\delta_0 + V_\infty \cos\delta_0 (x'_d + x_e)] + \frac{V_q}{V_t}[x'_d(r_e V_\infty \cos\delta_0 - V_\infty(x_q + x_e)\sin\delta_0)]\right\} \tag{A14}$$

$$K_6 = \frac{1}{\Delta}\left\{\frac{V_d}{V_t} x_q r_e - \frac{V_q}{V_t} x'_d (x_q + x_e)\right\} + \frac{V_q}{V_t} \tag{A15}$$

References

1. Mak, K.H.; Holland, B.L. Migrating electrical power network SCADA systems to TCP/IP and Ethernet networking. *Power Eng. J.* **2002**, *16*, 305–311.
2. Naduvathuparambil, B.; Valenti, M.C.; Feliachi, A. Communication delays in wide area measurement systems. In Proceedings of the Thirty-Fourth Southeastern Symposium on System Theory (Cat. No.02EX540), Huntsville, AL, USA, 19 March 2002; pp. 118–122.
3. Holbert, K.E.; Heydt, G.I.; Hui, N. Use of satellite technologies for power system measurements, command, and control. *Proc. IEEE* **2005**, *93*, 947–955. [CrossRef]
4. Li, M.; Chen, Y. A Wide-Area Dynamic Damping Controller Based on Robust H∞ Control for Wide-Area Power Systems With Random Delay and Packet Dropout. *IEEE Trans. Power Syst.* **2018**, *33*, 4026–4037. [CrossRef]
5. Khalil, A.; Wang, J. Stabilization of load frequency control system under networked environment. In Proceedings of the 2015 21st International Conference on Automation and Computing (ICAC), Glasgow, UK, 11–12 September 2015; pp. 1–6.
6. Khalil, A.; Wang, J.; Mohammed, O. Robust stabilization of load frequency control system under networked environment. *Int. J. Autom. Comput.* **2017**, *14*, 93–105. [CrossRef]
7. Wu, H.; Tsakalis, K.S.; Heydt, G.T. Evaluation of time delay effects to wide-area power system stabilizer design. *IEEE Trans. Power Syst.* **2004**, *19*, 1935–1941. [CrossRef]
8. Kamwa, I.; Grondin, R.; Hebert, Y. Wide-area measurement based stabilizing control of large power systems-a decentralized/hierarchical approach. *IEEE Trans. Power Syst.* **2001**, *16*, 136–153. [CrossRef]
9. Chaudhuri, B.; Majumder, R.; Pal, B.C. Wide-area measurement-based stabilizing control of power system considering signal transmission delay. *IEEE Trans. Power Syst.* **2004**, *19*, 1971–1979. [CrossRef]
10. Bhowmik, S.; Tomsovic, K.; Bose, A. Communication Models for Third Party Load Frequency Control. *IEEE Trans. Power Syst.* **2004**, *19*, 543–548. [CrossRef]
11. Ramakrishnan, K. Delay-dependent stability criterion for delayed load frequency control systems. In Proceedings of the 2016 IEEE Annual India Conference (INDICON), Bangalore, India, 16–18 December 2016; pp. 1–6.
12. Ramakrishnan, K.; Ray, G. Improved results on delay dependent stability of LFC systems with multiple time delays. *J. Control Autom. Electr. Syst.* **2015**, *2015*, 235–240. [CrossRef]
13. Jiang, L.; Yao, W.; Wu, Q.H.; Wen, J.Y.; Cheng, S.J. Delay-Dependent Stability for Load Frequency Control with Constant and Time-Varying Delays. *IEEE Trans. Power Syst.* **2012**, *27*, 932–941. [CrossRef]
14. Zhang, C.K.; Jiang, L.; Wu, Q.H.; He, Y.; Wu, M. Delay-Dependent Robust Load Frequency Control for Time Delay Power Systems. *IEEE Trans. Power Syst.* **2013**, *28*, 2192–2201. [CrossRef]

15. Zhang, C.K.; Jiang, L.; Wu, Q.H.; He, Y.; Wu, M. Further Results on Delay-Dependent Stability of Multi-Area Load Frequency Control. *IEEE Trans. Power Syst.* **2013**, *28*, 4465–4474. [CrossRef]
16. Xiaofeng, Y.; Tomsovic, K. Application of linear matrix inequalities for load frequency control with communication delays. *IEEE Trans. Power Syst.* **2004**, *19*, 1508–1515.
17. Sönmez, Ş.; Ayasun, S.; Nwankpa, C.O. An Exact Method for Computing Delay Margin for Stability of Load Frequency Control Systems with Constant Communication Delays. *IEEE Trans. Power Syst.* **2016**, *31*, 370–377. [CrossRef]
18. Jia, H.J.; Na, G.Y.; Lee, S.; Zhang, P. Study on the impact of time delay to power system small signal stability. In Proceedings of the MELECON 2006—2006 IEEE Mediterranean Electrotechnical Conference, Malaga, Spain, 16–19 May 2006; pp. 1011–1014.
19. Jia, H.; Cao, X.; Yu, X.; Zhang, P. A Simple Approach to Determine Power System Delay Margin. In Proceedings of the 2007 IEEE Power Engineering Society General Meeting, Tampa, FL, USA, 24–28 June 2007; pp. 1–7.
20. Jia, H.; Yu, X.; Yu, Y.; Wang, C. Power system small signal stability region with time delay. *Electr. Power Energy Syst.* **2008**, *30*, 16–22. [CrossRef]
21. Ayasun, S. Computation of time delay margin for power system small-signal stability. *Eur. Trans. Electr. Power* **2009**, *2009*, 949–968. [CrossRef]
22. Yu, X.; Jia, H.; Wang, C. CTDAE & CTODE models and their applications to power system stability analysis with time delays. *Sci. China Technol. Sci.* **2013**, *56*, 1213–1223.
23. Jiang, Y.; Jiang, T.; Jia, H.; Dong, C.Y. A novel LMI criterion for power system stability with multiple time-delays. *Sci. China Technol. Sci.* **2014**, *57*, 1392–1400. [CrossRef]
24. Dong, C.; Jia, H.; Jiang, T.; Bai, L.; Hu, Q.; Wang, L.; Jiang, Y. Effective method to determine time-delay stability margin and its application to power systems. *Iet Gener. Transm. Distrib.* **2017**, *11*, 1661–1670. [CrossRef]
25. Sonmez, S.; Ayasun, S. Effect of load increase and power system stabilizer on stability delay margin of a generator excitation control system. *Turkish J. Electr. Eng. Comput. Sci.* **2016**, *24*, 5183–5194. [CrossRef]
26. Chen, J. On Computing the Maximal Delay Intervals for Stability of Linear Delay Systems. *IEEE Trans. Autom. Control* **1995**, *40*, 1087–1093. [CrossRef]
27. Gu, K.; Kharitonov, V.L.; Chen, J. *Stability of Time-Delay Systems*; Springer: Berlin, Germany, 2003.
28. Chen, J.; Latchman, H.A. Frequency Sweeping Tests for Stability Independent of Delay. *IEEE Trans. Autom. Control* **1995**, *40*, 1640–1645. [CrossRef]
29. Chen, J.; Gu, G.; Nett, C.N. A New Method for Computing Delay Margins for Stability of Linear Delay Systems. In Proceedings of the 1994 33rd IEEE Conference on Decision and Control, Lake Buena Vista, FL, USA, 14–16 December 1994; pp. 433–437.
30. Shahgholian, G.; Faiz, J. The effect of power system stabilizer on small-signal stability in single-machine-innite-bus. *Int. J. Electr. Power Eng.* **2010**, *2010*, 45–53. [CrossRef]
31. Sauer, P.W.; Pai, M.A. *Power System Dynamics and Stability*, 1st ed.; Stipes Publishing: Singapore, 2002.
32. de Mello, F.P.; Laskowski, T.F. Concepts of power system dynamic stability. *IEEE Trans. Power Appar. Syst.* **1975**, *94*, 827–833. [CrossRef]
33. Heffron, W.G.; Phillips, R.A. Effect of a Modern Amplidyne Voltage Regulator on Underexcited Operation of Large Turbine Generators. Transactions of the American Institute of Electrical Engineers. *Part III Power Appar. Syst.* **1952**, *71*, 692–697. [CrossRef]
34. Demello, F.P.; Concordia, C. Concepts of synchronous machine stability as affected by excitation control. *IEEE Trans. Power Appar. Syst. Pas* **1969**, *88*, 316–329. [CrossRef]
35. Ji, W.; Venkatasubramanian, V. Hard-limit induced chaos in a fundamental power system model. *Electr. Power Energy Syst.* **1996**, *18*, 279–295. [CrossRef]